

FILA: FINE-GRAINED VISION LANGUAGE MODELS

Shiding Zhu^{1*}, Wenhui Dong^{2*}, Jun Song^{2†}, Yingbo Wang², Yanan Guo³, Bo Zheng²

¹Zhejiang University, ²Taobao & Tmall Group of Alibaba, ³USTC

ABSTRACT

Recently, there has been growing interest in the capability of multimodal large language models (MLLMs) to process high-resolution images. A common approach currently involves dynamically cropping the original high-resolution image into smaller sub-images, which are then fed into a vision encoder that was pre-trained on lower-resolution images. While this method enables MLLMs to process high-resolution images within input constraints, it often causes semantic fragmentation by truncating objects and connected areas, leading to degraded model performance, particularly for fine-grained details and irregularly shaped objects. To address this limitation, we propose FILA (Fine-Grained Vision Language Model), a novel framework designed to process images of high resolution while retaining the overall context during encoding. Specifically, we: (i) Introduce a Hybrid Encoder that not only encodes individual sub-images but also interacts with detailed global visual features, significantly improving the model’s ability to encode high-resolution images. (ii) Propose an effective feature fusion strategy for the dynamic cropping approach, effectively leveraging information from different layers of the vision encoder. Compared with the state-of-the-art MLLMs under the same setting, our FILA outperforms existing MLLMs in nine out of ten tasks. Specifically, FILA achieves a 9.6% improvement in performance on the TextVQA task and a 6.9% enhancement on the DocVQA task.

1 INTRODUCTION

Inspired by the remarkable achievements of large language models (LLMs) (Zhang et al., 2022; Brown et al., 2020; Touvron et al., 2023), the development of multimodal large language models (MLLMs) (Alayrac et al., 2022; Bai et al., 2023; Chen et al., 2024b; Li et al., 2023; Zhu et al., 2023; Liu et al., 2024a) is advancing at a rapid pace. Researchers have directed substantial efforts towards broadening the capabilities of LLMs to encompass additional modalities, resulting in significant breakthroughs in assorted vision-language tasks. Nevertheless, the challenge of fine-grained visual recognition is not adequately addressed. This shortcoming arises partly from the constraints inherent in pre-trained visual encoders (Zhai et al., 2023; Radford et al., 2021), which often require MLLMs to process images at relatively low resolutions, typically around 224×224 (Zhu et al., 2023; Ye et al., 2024) or 336×336 (Liu et al., 2024b). This limitation hinders the precise identification of fine details and contextual elements within images, resulting in less accurate vision understanding and reasoning.

To solve this limitation, recent endeavors are directed toward enabling MLLMs to handle images of high resolution. One approach involves directly utilizing a visual encoder designed to process higher-resolution images. However, this approach necessitates the training of a high-quality visual encoder, which requires significant computational resources, including high-quality, high-resolution training datasets. An alternative effective strategy is dynamic cropping (Ye et al., 2023; Li et al., 2024b; Xu et al., 2024; Hu et al., 2024; Liu et al., 2024d;b), where the high-resolution image is partitioned into a set of lower-resolution sub-images using adaptive algorithms. These segmented sub-images are subsequently processed by a visual encoder that has been previously trained with lower-resolution image data, thereby augmenting the encoder’s ability to capture finer details while ensuring that maintaining computational efficiency. Nevertheless, this cropping method can result

*Equal contribution

†Corresponding author

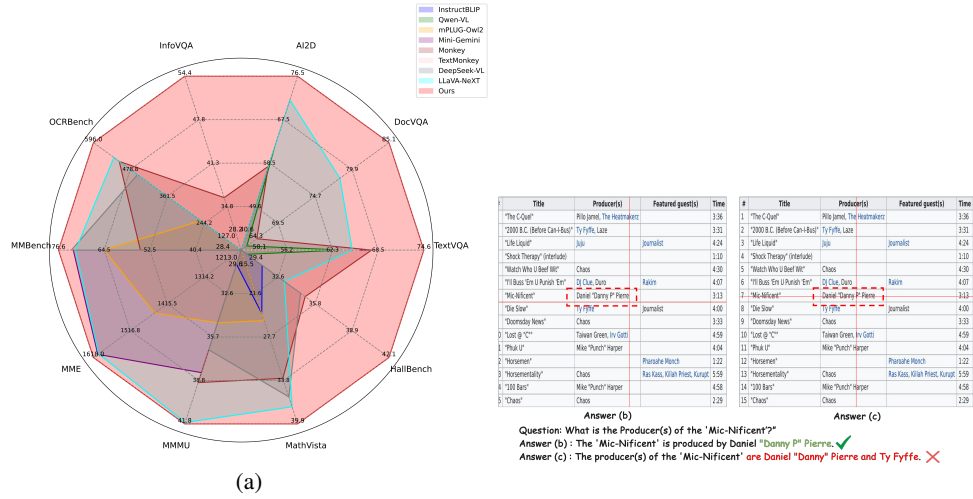


Figure 1: (a) An overall performance comparison between FILA and other existing MLLMs. (b) and (c) are examples of image fragments. The solid red line in the figures represents the cropping boundary. LLaVA-NeXT provides correct answers when pivotal information remains within the cropping boundaries. However, even slight overlaps with the boundaries cause it to misidentify the information.

in image fragmentation, thereby altering the original spatial context and disrupting positional associations within the image. This becomes particularly problematic when essential information is located at the edges of these cropped segments, as it poses challenges to encoding such information accurately. For instance, as depicted in Figure 1 when the pivotal information does not intersect with the cropping boundaries, the model LLaVA-NeXT (Liu et al., 2024b) provides the correct answer. However, with a slight alteration in the image such that the pivotal information intersects with the cropping boundaries, LLaVA-NeXT fails to identify it correctly.

To alleviate this effect, in this paper, we propose FILA enhancing fine-grained recognition. First, we design a visual encoder, Hybrid Encoder, under the dynamic cropping strategy to address the issue of image fragmentation. Hybrid Encoder can acquire comprehensive global information to enhance the encoding of each sub-image. Furthermore, we propose a different way of visual feature interaction called ConvNeXt-ViT Deep Fusion Module (CVFM), which fully utilizes features at different levels for mutual complementarity, achieving optimal visual encoding.

Figure 2 demonstrates the difference between our approach and previous methods. Previous methods include Dynamic Resolution, Mini-Gemini (Li et al., 2024a), and Channel-wise Concat. Dynamic Resolution simply involves cropping the image and feeding it into CLIP-ViT (Dosovitskiy, 2020). Mini-Gemini interacts the low-resolution CLIP-ViT features with a high-resolution auxiliary branch at the last layer, mainly using Cross Attention, while some methods utilize Channel-wise Concat. The innovation of our method lies in our interaction between two high-resolution branches and the novel idea of deep fusion, which successfully addresses the issue of image fragmentation.

To verify the effectiveness of our proposed method, we conducted extensive experiments on ten vision-language tasks, some of which include fine-grained recognition of high-resolution images, such as TextVQA (Singh et al., 2019) and DocVQA (Mathew et al., 2021b). The experimental results show that our method outperforms existing MLLMs on 9 out of 10 Vision-Language tasks. Specifically, it surpasses LLaVA-NeXT by 9.6% on TextVQA and by 6.9% on DocVQA.

In summary, our contributions are three folds:

- We propose a new visual encoder, Hybrid Encoder, to solve the problem of image fragmentation under dynamic cropping strategies. Hybrid Encoder can utilize comprehensive global information to enhance sub-image encoding, improving the model’s upper limit in handling high-resolution images.

- We design a novel visual feature fusion module CVFM, cleverly utilizing information at different levels for mutual complementarity.
- Based on our strategy, we developed the FILA model, a powerful MLLM that outperforms existing models on multiple benchmarks, demonstrating the effectiveness of our approach.

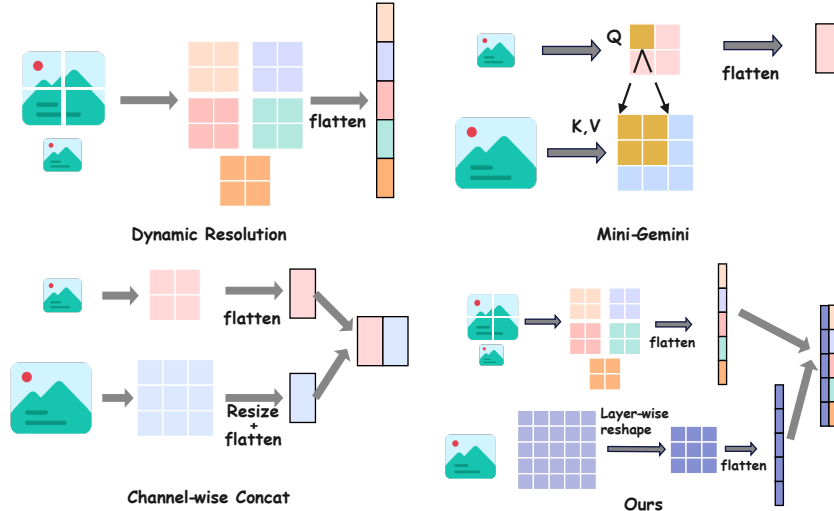


Figure 2: An Overview of High-Resolution Methods. This Figure illustrates the differences between our method and previous methods.

2 RELATED WORK

2.1 LARGE VISION-LANGUAGE MODEL

Driven by the tremendous success of large language models (LLMs), there has been growing interest in building end-to-end multimodal large language models. Specifically, most existing MLLMs adopt a modular structure, utilizing an intermediate network to project visual features into the word embedding space of an LLM. Then, the LLM completes various vision-language (VL) tasks in an autoregressive manner. The intermediate networks of existing MLLMs can generally be divided into two types: (i) learned queries, such as perceiver resamplers (Alayrac et al., 2022) or Q-Formers (Li et al., 2023), which use fixed queries to capture features through cross-attention; and (ii) MLP modules, like those in the LLaVA series (Liu et al., 2024a; 2023a). The vision encoder functions as the “eye” of the model, allowing it to interpret and examine visual information. This encoder can incorporate different architectures, like the Vision Transformer (ViT) (Vaswani, 2017) or ConvNeXt (Liu et al., 2022) which have been used in image classification and object detection (Zheng et al., 2023). A majority of MLLMs use CLIP-ViT as the vision encoder, which is trained on large image-text datasets, to proficiently extract visual features. However, CLIP-ViT is pretrained on low-resolution images and cannot directly handle high-resolution images, which limits the model’s performance on fine-grained tasks.

2.2 HIGH-RESOLUTION MLLMS

Directly inputting high-resolution images into visual encoders leads to high computational costs, primarily due to the quadratic complexity associated with the Transformer architecture and the substantial increase in the number of visual tokens. To alleviate this issue, existing high-resolution MLLMs can be divided into two main types. One type adopts a dynamic cropping method, cutting images into patches that are then separately input into Vision Transformers (ViTs) trained on low-resolution images. Although this method is simple and efficient, it can lead to the problem of image fragmentation, altering the original context, and disrupting positional relationships. In particular, if

key information is located at the boundaries of the cropped images, it becomes difficult to encode it accurately. The other (Wei et al., 2023; Zhang et al., 2024; Hong et al., 2023) type uses a dual-encoder approach, introducing a high-resolution branch to supplement the low-resolution branch. For example, Vary (Wei et al., 2023) and Deepseek-VL (Lu et al., 2024a) utilize the Segment Anything Model (SAM) (Kirillov et al., 2023) in the high-resolution visual encoder to better capture detailed information, while MiniGemini (Li et al., 2024a) and LLaVA-HR (Luo et al., 2024) adopt ConvNeXt. However, the main visual encoder in these models is still CLIP-ViT, whose capabilities are limited by its low resolution. In our work, we designed a visual encoder called Hybrid Encoder specifically for the dynamic cropping strategy. Hybrid Encoder expands the ability of CLIP-ViT to process high-resolution images, solving the problem of image fragmentation and improving the model’s capacity to handle high-resolution images.

3 METHODOLOGY

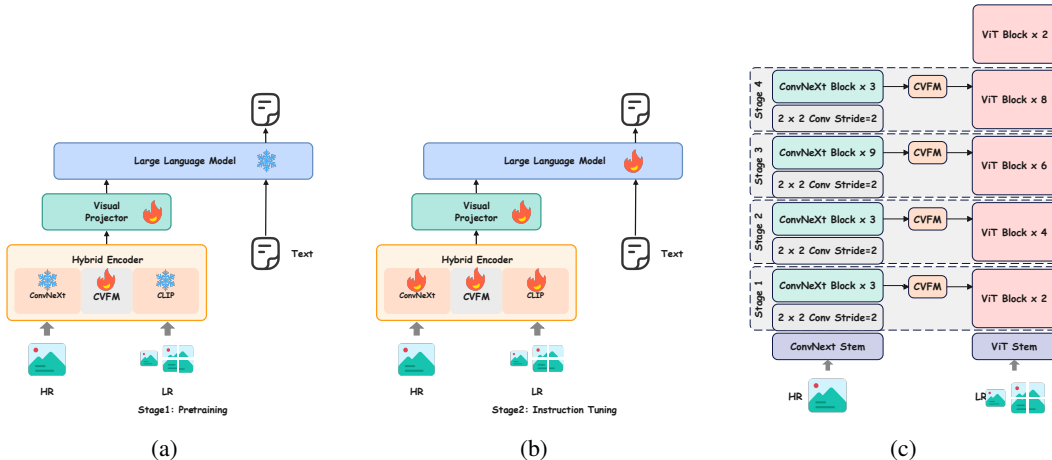


Figure 3: Whole architecture for MLLMs. (a) is the first stage of training, during which we only activate the CVFM and projector. (b) is the second stage of training, where we activate all modules of the model. (c) is the structural diagram of Hybrid Encoder, which features high-resolution branches working collaboratively.

Figure 3 provides an overview of FILA. Initially, the image is dynamically segmented, resulting in several sub-images, including the original low-resolution image. These sub-images are processed by our newly designed visual encoder, the Hybrid Encoder. After passing through a projection layer, the encoded visual features are integrated with the textual features and subsequently fed into the large language model (LLM). In Section 3.1 we briefly introduce the overall model architecture. Section 3.2 presents our newly designed visual encoder, the Hybrid Encoder. In Section 3.3, we describe our optimal fusion strategy, and Section 3.4 outlines the training paradigm for the FILA model.

3.1 MODEL ARCHITECTURE

We apply a dynamic segmentation method to partition the input image into smaller blocks while maintaining the original aspect ratio. The image is resized and padded to the most appropriate predefined resolution, then segmented into $n_w \times n_h$ patches, each sized 336×336 . The predefined resolutions are: 336×672 , 672×336 , 672×672 , 1008×336 , and 336×1008 .

To select the best resolution, we calculate the effective resolution (Res_{eff}) and the wasted resolution (Res_{wasted}) for each predefined resolution. The selection aims to maximize Res_{eff} and minimize

Res_{wasted} if multiple resolutions have the same Res_{eff} .

$$\text{Scale} = \min\left(\frac{W_h}{W_l}, \frac{H_h}{H_l}\right), \quad (1)$$

$$W_s, H_s = W_l \times \text{Scale}, H_l \times \text{Scale}, \quad (2)$$

$$Res_{eff} = \min(W_s \times H_s, W_l \times H_l), \quad (3)$$

$$Res_{wasted} = (W_h \times H_h) - Res_{eff}. \quad (4)$$

Here, W_h and H_h are the predefined high resolution dimensions, while W_l and H_l are the input image's width and height. Scale is used to resize the image proportionally. After resizing, Res_{eff} ensures it does not exceed the input image's resolution, and Res_{wasted} measures unused space. The predefined resolution with the highest Res_{eff} is chosen, and if multiple resolutions have the same Res_{eff} , the one with the least Res_{wasted} is selected.

In addition to the segmented patches, a global view of the image is created by resizing it to 336×336 , offering a complete overview. Both the global view and the patches are processed through a Hybrid Encoder to extract features, which are then aligned by an MLP and combined with text features. Finally, these features are input into a language decoder for the final predictions.

3.2 HYBRID ENCODER

The architecture of the proposed Hybrid Encoder is depicted in Figure 3c. This architecture integrates ConvNeXt, CLIP-ViT, and CVFM modules. Both the ConvNeXt and ViT networks are divided into four stages. The final layer of each stage serves as an interaction layer, combining its output with that of the corresponding ConvNeXt stage via the CVFM module. This design enables the acquisition of fine-grained global information and effectively mitigates image fragmentation.

In the dynamic cropping strategy, an optimal high-resolution setting $H_h \times W_h$ is selected. The original image I_l is resized and padded to a predefined resolution while preserving its aspect ratio. As a result, a low-resolution global image and a series of sub-images $[I^{global}, I_1^{loc}, I_2^{loc}, \dots, I_N^{loc}]$ are obtained for subsequent processing by the CLIP-ViT. In parallel, the original image I_l is also resized and padded to a higher resolution of $(\frac{32}{14} \times H_h, \frac{32}{14} \times W_h)$. This high-resolution image I_h is directly encoded by ConvNeXt, yielding a set of multi-level high-resolution features $\mathbf{F}_{vh} = [\mathbf{F}_{vh}^1, \mathbf{F}_{vh}^2, \mathbf{F}_{vh}^3, \mathbf{F}_{vh}^4]$.

The choice of the $(\frac{32}{14} \times H_h, \frac{32}{14} \times W_h)$ resolution ensures that the image aspect ratio is maintained, allowing more detailed information to be captured. It also facilitates subsequent alignment with CLIP-ViT features. In particular, this configuration guarantees that the output dimensions of each ConvNeXt stage are integer multiples of the concatenated dimensions of all ViT hidden layer features, simplifying the alignment and dimensional transformations. Detailed dimensional operations are provided in Table 5. In this table, we use an input image of 336×336 as an example, and the cropping strategy dictates that the resolution of the image input to ConvNeXt is 768×768 .

During the encoding process in CLIP-ViT, the features of each sub-image interacts with a corresponding subset of \mathbf{F}_{vh} , thus incorporating enhanced contextual information and effectively addressing the fragmentation problem associated with conventional dynamic slicing methods. The specific mechanisms of these interactions are elaborated upon in the following section.

3.3 CONVNEXT-ViT DEEP FUSION MODULE (CVFM)

To enhance the interaction between ConvNeXt and CLIP-ViT features, we propose the ConvNeXt-ViT Deep Fusion Module (CVFM). The CVFM is designed to crop the overall features extracted by ConvNeXt to match the corresponding features of CLIP-ViT, concatenate them along the channel dimension, and integrate features from various stages of ConvNeXt into the encoding process of CLIP-ViT.

Initially, the features from each stage of ConvNeXt are resized to align with the feature dimensions of the hidden layers in CLIP-ViT. Consistent with the outcomes of dynamic cropping, the features from each stage, denoted as \mathbf{F}_{vh}^i , are segmented into global and multiple local components:

$$\mathbf{F}_{vh}^i = \left[\mathbf{F}_{vh-i}^{\text{global}}, \mathbf{F}_{vh-i}^{\text{loc1}}, \mathbf{F}_{vh-i}^{\text{loc2}}, \dots, \mathbf{F}_{vh-i}^{\text{locN}} \right]$$

In the interaction layer, the hidden layer features of CLIP-ViT are fused with the corresponding high-resolution features. Specifically, lower-level features interact with lower-level features, and higher-level features interact with higher-level features. The interaction is formalized as follows:

$$\mathbf{F}_{vl}^{i'} = \mathbf{F}_{vl}^i + \tanh(\alpha_{dense}) \cdot \text{MLP} \left(\mathbf{F}_{vl}^i \oplus \mathbf{F}_{vh}^{i'} \right), \quad (5)$$

where \mathbf{F}_{vl}^i represents the feature before the interaction layer of the i -th stage of CLIP-ViT, and $\mathbf{F}_{vh}^{i'}$ denotes the corresponding high-resolution feature. The \oplus operator signifies concatenation along the channel dimension. After passing through the multilayer perceptron (MLP), the number of channels is restored to match the original number of channels in CLIP-ViT. The parameter α_{dense} serves as a gating mechanism, initialized to zero to preserve the integrity of the visual model during initialization, thereby enhancing both stability and performance.

Although each CLIP-ViT interacts exclusively with its corresponding high-resolution feature, the convolutional properties of ConvNeXt enable each feature to effectively capture global information, thereby compensating for the limitation of each ViT, which is restricted to local sub-images. Additionally, the interaction layer provides ViT with more detailed features, resulting in a final visual representation that is both more accurate and comprehensive.

3.4 TRAINING PARADIGM

As shown in Figure 3, we adopted a two-stage approach in training FILA, which includes low-resolution pre-training and high-resolution visual instruction fine-tuning. The goal is to align visual features with the language model during the pre-training stage, followed by fine-tuning the language model in the instruction tuning stage. Specifically, during the pre-training phase, we do not use a dynamic cropping strategy; instead, we directly resize the images to 336×336 for I_l and 768×768 for I_h . We enable CVFM and the visual projector to train while keeping the other layers of the language model and Hybrid Encoder frozen. In the instruction fine-tuning stage, we employ a dynamic cropping strategy, and all parts of the model are trainable, including the ConvNeXt used for generating high-resolution features. The detail training setting as described in Section B.

4 EXPERIMENTS

4.1 IMPLEMENTATION

Datasets To achieve effective cross-modality alignment and instruction finetuning, we have gathered high-quality datasets from publicly accessible sources. Initially, we focus on pretraining the projector and interaction layers by amassing approximately 1.2M image captions. This includes 558K image-caption pairs extracted from the LLaVA-filtered CC3M dataset (Changpinyo et al., 2021) and 695K GPT-4V-generated captions from the ALLaVA dataset (Chen et al., 2024a). For instruction finetuning, diverse datasets are utilized: 643K single- and multi-turn conversations (minus 21K TextCaps data) from the LLaVA (Liu et al., 2023a) dataset, in addition to 100K QA pairs from ShareGPT4V (Chen et al., 2023), 10K LAION-GPT-4V captions (eV, 2023), 6K text-only multi-turn dialogues from LIMA (Zhou et al., 2023) and OpenAssistant2 (Köpf et al., 2024), and 700K GPT-4V-constructed instruction pairs from the ALLaVA dataset. To enhance OCR-related competencies, we further incorporate 28K QA pairs comprised of 10K DocVQA (Mathew et al., 2021b), 4K ChartQA (Masry et al., 2022), 10K DVQA (Kafle et al., 2018), and 4K AI2D (Kembhavi et al., 2016) data. Overall, our datasets support about 1.5M instruction-related conversations aimed at improving image comprehension.

4.2 EVALUATIONS

Benchmarks Following prior work, we evaluated our HyViLM on ten benchmarks. These include five general multimodal understanding benchmarks: MMBench (Liu et al., 2023b), MMMU (Yue et al., 2024), MME (Fu et al., 2023), MathVista (Lu et al., 2024b), and HallusionBench (Guan et al., 2024), as well as five document understanding-related benchmarks: TextVQA (Singh et al., 2019), DocVQA (Tito et al., 2021), AI2D (Kembhavi et al., 2016), InfoVQA (Mathew et al., 2021a), and OCRBench (Liu et al., 2024c). This selection was made to demonstrate that our model not only possesses strong fine-grained recognition abilities but also exhibits excellent general capabilities.

MLLMs We compared our model with some state-of-the-art multi-language large models (MLLMs). (1) Normal Resolution MLLMs, such as LLaVA1.5 (Liu et al., 2024a), InstructBLIP (Dai et al., 2023), Qwen-VL (Bai et al., 2023), and mPLUG-Owl2 (Ye et al., 2024). (2) High Resolution MLLMs, such as MiniGemini (Li et al., 2024a), CogAgent (Hong et al., 2023), Monkey (Li et al., 2024b), TextMonkey (Liu et al., 2024d), HiRes-LLaVA-336px (Huang et al., 2024), LLaVA-UHD (Xu et al., 2024), DocOwl-1.5-Chat (Hu et al., 2024), DeepSeek-VL (Lu et al., 2024a), MiniGemini-HD (Li et al., 2024a), and LLaVA-NeXT (Liu et al., 2024b).

4.3 MAIN RESULTS

Model	LLM	MaxRes	Doc					General			
			TextVQA	DocVQA	AI2D	InfoVQA	OCR Bench	MMBench	MME	MMMU	MathVista
Normal Resolution MLLMs											
LLaVA1.5	Vicuna-7B	336 × 336	58.2	-	54.8	-	-	64.3	1511/-	-	-
InstructBLIP	Vicuna-7B	224 × 224	50.1	-	40.6*	-	276*	28.4*	1213/-	30.6*	24.4*
Qwen-VL	Qwen-7B	448 × 448	63.8	65.1	62.3	-	127*	38.2	-	29.6*	15.5*
mPLUG-Owl2	LLaMA-7B	224 × 224	58.2	-	55.7*	-	255*	64.5	1450/-	34.7*	25.4*
High Resolution MLLMs											
MiniGemini	LLaMA3-8B	336(768)	67.2	-	-	-	-	72.7	1606/341	38.2	-
CogAgent	LLaMA2-7B	224(1120)	-	81.6	-	44.5	-	76.1	-	-	-
Monkey	Qwen-7B	1344 × 896	67.6	66.5	57.9	36.1	514*	55.0*	-	38.9*	33.5*
TextMonkey	Qwen-7B	896	65.9	64.3	-	28.2	561	-	-	-	-
HiRes-LLaVA-336px	Vicuna-7B	1344 × 1344	-	74.7	69.7	48.0	-	70.5	-	-	42.6
LLaVA-UHD	Vicuna-13B	672 × 1008	-	-	-	-	-	68	1535/-	-	-
DocOwl-1.5-Chat	7B	1344 × 1344	68.6	82.2	-	50.7	-	-	-	-	-
DeepSeek-VL	DeepSeek-LLM-7B	384(1024)	-	-	65.3*	-	456	73.2	-	36.6	36.1
MiniGemini-HD	LLaMA3-8B	672(1536)	71.6	-	-	-	-	-	1532/357	37.0	-
LLaVA-NeXT	LLaMA3-8B	672 × 672	65.0	78.2	71.6	-	531*	72.1	1604/368	41.7	37.5
HyViLM	LLaMA3-8B	672(1536)	74.6	85.1	76.5	54.4	596	76.6	1618/388	41.8	39.9

Table 1: Quantitative results on 10 popular benchmarks, including 5 general benchmarks and 5 document understanding-related benchmarks. “MaxRes” means the maximum resolution supported. The meaning of “672(1536)” is to integrate features of an image with a resolution of 1536×1536 into features of an image with a resolution of 672×672 . * means that the metric is provided by OpenCompass (Contributors, 2023).

General Multimodal Understanding We evaluated HyViLM in terms of general multimodal understanding, and the results are shown in Table 1. Our model exceeds the vast majority of models of comparable size. In particular, on MME, we surpass LLaVA-NeXT by 1.7% and MiniGemini-HD by 6.2%. MiniGemini-HD also employs the ConvNeXt visual encoder, with a maximum image resolution consistent with ours, and the training data are almost identical to ours, highlighting the superiority of our approach compared to Minigemini. On MathVista, we significantly outperform the best model, LLaVA-NeXT, by 6.4%. Furthermore, on three additional general benchmarks, MMBench, MMMU and HallBench, we also achieved SOTA or near-SOTA results. It is evident that our approach greatly enhances the general understanding capabilities of MLLMs.

Document Understanding We have achieved outstanding performance on document-related leaderboards, making significant advancements in five document understanding tasks. Compared to the state-of-the-art models, HyViLM outperforms by 4.2% on TextVQA, 3.5% on DocVQA, 6.8% on AI2D, 7.3% on InfoVQA, and 6.2% on OCRBench. Additionally, our input tokens to the LLM remain consistent with LLaVA-NeXT, resulting in a substantial performance boost while maintaining computational complexity. It is noteworthy that MiniGemini-HD is a variant of our model that only enables shallow interactions of different visual features, highlighting the importance of deep visual feature interactions under a dynamic cropping strategy. Therefore, we can conclude that our designed Hybrid Encoder significantly enhances the model’s fine-grained recognition capability.

4.4 ABLATION STUDIES

In this section, we conduct ablation experiments on our model to fully validate its effectiveness. We use TextVQA, InfoVQA, MME for the ablation study.

Impact of Image Fragmentation To validate our point that the dynamic slicing strategy can lead to image fragmentation, we compared our method with several alternatives: simply using dynamic

Method	TextVQA	InfoVQA	MME
DS	71.4	46.7	2000
DS + Channle Concat	71.0	50.0	1989
DS + Local Cross Attetion	73.2	50.6	2043
DS + Global Cross Attetion	71.5	47.4	2000
DS + Hybrid Encoder	74.6	54.4	2006

Table 2: The Impact of Image Fragmentation on the Model. Except for Hybrid Encoder, the other feature interactions in the table occur in the final layer of the ViT. “DS” stands for dynamic slicing.

Conv Layer	ViT Layer	TextVQA	InfoVQA	MME
Multi Layers	2	73.5	54.02	2001
Multi Layers	6	73.9	53.3	2020
Last Layer	4	73.7	53.4	2019
Pyramid Fusion	4	73.7	53.6	1993
Multi Layers	4	74.6	54.4	2006

Table 3: Ablation study of the optimal interaction structure. “Multi Layers” refers to the interaction between lower- and higher-level features of ConvNeXt and ViT. “Last Layer” uses only the final layer features of ConvNeXt for interaction. “Pyramid Fusion” fuses multi-level features of ConvNeXt before interacting with ViT. “ViT Layer” indicates the number of interaction layers in ViT.

slicing to improve model resolution, and a variant of our model that combines dynamic slicing with feature interaction between CLIP-ViT and ConvNeXt at the last layer. Interaction methods include channel-wise concatenation, local cross-attention, and global cross-attention. Local cross-attention means that each feature of CLIP-ViT only interacts with its corresponding feature from ConvNeXt, whereas global cross-attention means that each feature of CLIP-ViT interacts with all features from ConvNeXt. We trained using the same complete dataset. As shown in Table 2, our model significantly outperforms the dynamic slicing approach. Compared to dynamic slicing with last-layer interaction, our model also shows a noticeable advantage, which rules out the impact of ConvNeXt on model performance. It also indicates that the issue of image fragmentation occurs during the encoding process of CLIP-ViT, and that performing feature interaction after encoding offers limited performance improvement. These experiments clearly demonstrate that it’s necessary to alter the internal structure of CLIP-ViT, so it becomes an integrated whole capable of encoding high-resolution images holistically.

The Optimal Interaction Structure In Table 3, we conducted ablation experiments to explore the optimal interaction structure. As shown in Table 2, using only the output from the last layer of ConvNeXt for interaction features provides limited additional information and proves to be suboptimal. Therefore, we designed a multi-layer to multi-layer interaction scheme, where the lower-layer features of ConvNeXt interact with the shallow-layer features of CLIP, and the deep-layer features of ConvNeXt interact with the deep-layer features of CLIP. We believe that this approach allows the CLIP model to gradually integrate into the ConvNeXt features while maintaining feature alignment. We also explored a pyramid-like approach, where we first fused multiple layers of features from ConvNeXt before interacting with CLIP-ViT, but the results were not satisfactory. On top of this, we also varied the number of interaction layers and found that four layers are optimal. The performance of the model declines with two or six layers. We believe that too few interaction layers cannot solve the issue of image fragmentation, while too many layers disrupt the excellent encoding capabilities of the original CLIP-ViT.

Ablation Study of Interaction Methods The above ablation study demonstrates that utilizing multi-level information from ConvNeXt to interact with CLIP-ViT yields the best results. The following ablation experiments investigate different fusion methods. We designed the experiments as follows: in the CVFM, we used channel concatenation, local cross attention, global cross attention, and feature addition as fusion methods. It can be seen that the channel concatenation method produced the best results. This method requires resizing the features from different levels of ConvNeXt to

Resize Method	Int. Mode	TextVQA	InfoVQA	MME
Interp	Local CA	72.8	50.0	1980
Interp	Global CA	71.3	49.0	1997
Interp	Add	73.9	53.3	2045
Conv	Channel	74.4	54.9	1973
Interp	Channel	74.6	54.4	2006

Table 4: Ablation Study of Interaction Methods. **Int. Mode** means the interaction mode between ViT and ConvNeXt in CVMF, and **CA** refers to Cross Attention. Note that the experiments here are all based on deep feature interactions.

match the feature dimensions of CLIP-ViT. We compared interpolation and convolution as resizing methods and found that interpolation achieves slightly better performance than convolution.

4.5 QUALITATIVE ANALYSIS

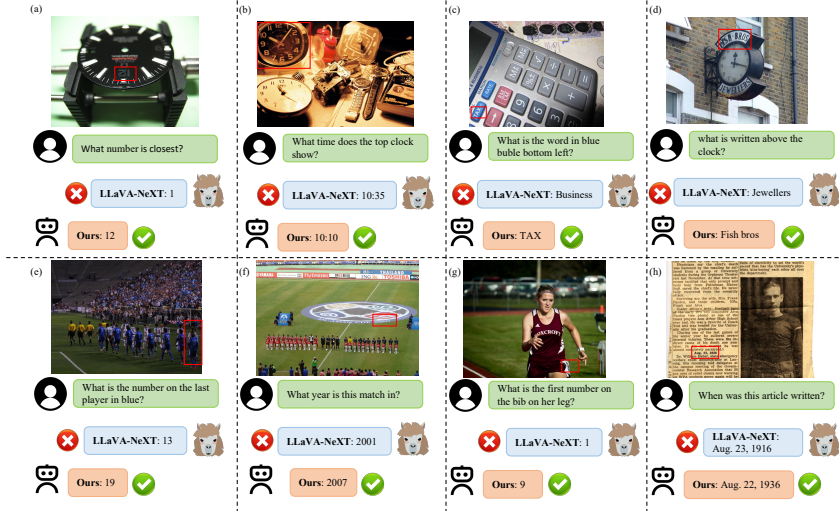


Figure 4: Qualitative Analysis. The issue of image fragmentation has been greatly reduced after incorporating Hybrid Encoder.

In Figure 4, we compare the prediction results of HyViLM with LLaVA-NeXT, where LLaVA-NeXT is trained with the same data. Our model has made advancements on three levels: recognition of critical information near the cropped boundaries, judgment of positional relationships, and detail recognition capability. In the example (a), the correct answer “12” was split into two sub-images, causing LLaVA-NeXT to make a mistake and only answer “1”, while our model answered correctly. In the example (d), due to dynamic image cropping, LLaVA-NeXT misjudged the positional relationship of top and bottom, as the question required the text on the clock to be answered, but it responded with the text below the clock. In the example (h), our model accurately recognized very fine-grained information and was entirely correct, whereas LLaVA-NeXT only partially succeeded in recognizing the information. These results further validate the effectiveness of Hybrid Encoder in addressing image fragmentation and improving the model’s fine-grained recognition capability.

5 CONCLUSION

In this article, we introduce a novel visual encoder, Hybrid Encoder, under a dynamic partitioning strategy. Hybrid Encoder addresses the fragmentation issue in images effectively by altering the structure of CLIP-ViT and incorporating global and fine-grained features using the CVMF approach.

The model HyViLM, which applies Hybrid Encoder, achieves state-of-the-art performance in extensive experiments, including both document-related benchmarks and various general benchmarks. Notably, HyViLM is the first study to explore the collaboration of two high-resolution branches, offering a new perspective for further enhancing the fine-grained recognition capabilities of MLLMs.

REFERENCES

Jean-Baptiste Alayrac, Jeff Donahue, Pauline Luc, Antoine Miech, Iain Barr, Yana Hasson, Karel Lenc, Arthur Mensch, Katherine Millican, Malcolm Reynolds, et al. Flamingo: a visual language model for few-shot learning. *Advances in neural information processing systems*, 35:23716–23736, 2022.

Jinze Bai, Shuai Bai, Shusheng Yang, Shijie Wang, Sinan Tan, Peng Wang, Junyang Lin, Chang Zhou, and Jingren Zhou. Qwen-vl: A frontier large vision-language model with versatile abilities. *arXiv preprint arXiv:2308.12966*, 2023.

Tom B. Brown, Benjamin Mann, Nick Ryder, Melanie Subbiah, Jared Kaplan, Prafulla Dhariwal, Arvind Neelakantan, Pranav Shyam, Girish Sastry, Amanda Askell, Sandhini Agarwal, Ariel Herbert-Voss, Gretchen Krueger, Tom Henighan, Rewon Child, Aditya Ramesh, Daniel M. Ziegler, Jeffrey Wu, Clemens Winter, Christopher Hesse, Mark Chen, Eric Sigler, Mateusz Litwin, Scott Gray, Benjamin Chess, Jack Clark, Christopher Berner, Sam McCandlish, Alec Radford, Ilya Sutskever, and Dario Amodei. Language models are few-shot learners, 2020. URL <https://arxiv.org/abs/2005.14165>.

Soravit Changpinyo, Piyush Sharma, Nan Ding, and Radu Soricut. Conceptual 12m: Pushing web-scale image-text pre-training to recognize long-tail visual concepts, 2021. URL <https://arxiv.org/abs/2102.08981>.

Guiming Hardy Chen, Shunian Chen, Ruifei Zhang, Junying Chen, Xiangbo Wu, Zhiyi Zhang, Zhi-hong Chen, Jianquan Li, Xiang Wan, and Benyou Wang. Allava: Harnessing gpt4v-synthesized data for lite vision-language models, 2024a. URL <https://arxiv.org/abs/2402.11684>.

Lin Chen, Jinsong Li, Xiaoyi Dong, Pan Zhang, Conghui He, Jiaqi Wang, Feng Zhao, and Dahua Lin. Sharegpt4v: Improving large multi-modal models with better captions, 2023. URL <https://arxiv.org/abs/2311.12793>.

Zhe Chen, Jiannan Wu, Wenhui Wang, Weijie Su, Guo Chen, Sen Xing, Muyan Zhong, Qinglong Zhang, Xizhou Zhu, Lewei Lu, et al. Internvl: Scaling up vision foundation models and aligning for generic visual-linguistic tasks. In *Proceedings of the IEEE/CVF Conference on Computer Vision and Pattern Recognition*, pp. 24185–24198, 2024b.

OpenCompass Contributors. Opencompass: A universal evaluation platform for foundation models. <https://github.com/open-compass/opencompass>, 2023.

Wenliang Dai, Junnan Li, Dongxu Li, Anthony Meng Huat Tiong, Junqi Zhao, Weisheng Wang, Boyang Li, Pascale Fung, and Steven Hoi. Instructblip: Towards general-purpose vision-language models with instruction tuning. *arXiv:2305.06500*, 2023.

Alexey Dosovitskiy. An image is worth 16x16 words: Transformers for image recognition at scale. *arXiv preprint arXiv:2010.11929*, 2020.

LAION eV. Laion/gpt4v-dataset · datasets at hugging face, 2023. URL <https://huggingface.co/datasets/laion/gpt4v-dataset>.

Chaoyou Fu, Peixian Chen, Yunhang Shen, Yulei Qin, Mengdan Zhang, Xu Lin, Zhenyu Qiu, Wei Lin, Jinrui Yang, Xiawu Zheng, et al. Mme: A comprehensive evaluation benchmark for multi-modal large language models. *arXiv:2306.13394*, 2023.

Tianrui Guan, Fuxiao Liu, Xiyang Wu, Ruiqi Xian, Zongxia Li, Xiaoyu Liu, Xijun Wang, Lichang Chen, Furong Huang, Yaser Yacoob, Dinesh Manocha, and Tianyi Zhou. Hallusionbench: An advanced diagnostic suite for entangled language hallucination and visual illusion in large vision-language models, 2024. URL <https://arxiv.org/abs/2310.14566>.

Wenyi Hong, Weihan Wang, Qingsong Lv, Jiazheng Xu, Wenmeng Yu, Junhui Ji, Yan Wang, Zihan Wang, Yuxuan Zhang, Juanzi Li, Bin Xu, Yuxiao Dong, Ming Ding, and Jie Tang. Cogagent: A visual language model for gui agents, 2023. URL <https://arxiv.org/abs/2312.08914>.

Anwen Hu, Haiyang Xu, Liang Zhang, Jiabo Ye, Ming Yan, Ji Zhang, Qin Jin, Fei Huang, and Jingren Zhou. mplug-docowl2: High-resolution compressing for ocr-free multi-page document understanding. *arXiv preprint arXiv:2409.03420*, 2024.

Runhui Huang, Xinpeng Ding, Chunwei Wang, Jianhua Han, Yulong Liu, Hengshuang Zhao, Hang Xu, Lu Hou, Wei Zhang, and Xiaodan Liang. Hires-llava: Restoring fragmentation input in high-resolution large vision-language models, 2024. URL <https://arxiv.org/abs/2407.08706>.

Kushal Kafle, Brian Price, Scott Cohen, and Christopher Kanan. Dvqa: Understanding data visualizations via question answering, 2018. URL <https://arxiv.org/abs/1801.08163>.

Aniruddha Kembhavi, Mike Salvato, Eric Kolve, Minjoon Seo, Hannaneh Hajishirzi, and Ali Farhadi. A diagram is worth a dozen images. In *ECCV*, 2016.

Alexander Kirillov, Eric Mintun, Nikhila Ravi, Hanzi Mao, Chloe Rolland, Laura Gustafson, Tete Xiao, Spencer Whitehead, Alexander C. Berg, Wan-Yen Lo, Piotr Dollár, and Ross Girshick. Segment anything, 2023. URL <https://arxiv.org/abs/2304.02643>.

Andreas Köpf, Yannic Kilcher, Dimitri von Rütte, Sotiris Anagnostidis, Zhi Rui Tam, Keith Stevens, Abdullah Barhoum, Duc Nguyen, Oliver Stanley, Richárd Nagyfi, et al. Openassistant conversations-democratizing large language model alignment. *Advances in Neural Information Processing Systems*, 36, 2024.

Junnan Li, Dongxu Li, Silvio Savarese, and Steven Hoi. Blip-2: Bootstrapping language-image pre-training with frozen image encoders and large language models. In *International conference on machine learning*, pp. 19730–19742. PMLR, 2023.

Yanwei Li, Yuechen Zhang, Chengyao Wang, Zhisheng Zhong, Yixin Chen, Ruihang Chu, Shaoteng Liu, and Jiaya Jia. Mini-gemini: Mining the potential of multi-modality vision language models, 2024a. URL <https://arxiv.org/abs/2403.18814>.

Zhang Li, Biao Yang, Qiang Liu, Zhiyin Ma, Shuo Zhang, Jingxu Yang, Yabo Sun, Yuliang Liu, and Xiang Bai. Monkey: Image resolution and text label are important things for large multi-modal models. In *Proceedings of the IEEE/CVF Conference on Computer Vision and Pattern Recognition*, pp. 26763–26773, 2024b.

Haotian Liu, Chunyuan Li, Qingyang Wu, and Yong Jae Lee. Visual instruction tuning, 2023a. URL <https://arxiv.org/abs/2304.08485>.

Haotian Liu, Chunyuan Li, Yuheng Li, and Yong Jae Lee. Improved baselines with visual instruction tuning, 2024a. URL <https://arxiv.org/abs/2310.03744>.

Haotian Liu, Chunyuan Li, Yuheng Li, Bo Li, Yuanhan Zhang, Sheng Shen, and Yong Jae Lee. Llava-next: Improved reasoning, ocr, and world knowledge, 2024b.

Yuan Liu, Haodong Duan, Yuanhan Zhang, Bo Li, Songyang Zhang, Wangbo Zhao, Yike Yuan, Jiaqi Wang, Conghui He, Ziwei Liu, et al. Mmbench: Is your multi-modal model an all-around player? *arXiv:2307.06281*, 2023b.

Yuliang Liu, Zhang Li, Mingxin Huang, Biao Yang, Wenwen Yu, Chunyuan Li, Xucheng Yin, Chenglin Liu, Lianwen Jin, and Xiang Bai. Ocrbench: On the hidden mystery of ocr in large multimodal models, 2024c. URL <https://arxiv.org/abs/2305.07895>.

Yuliang Liu, Biao Yang, Qiang Liu, Zhang Li, Zhiyin Ma, Shuo Zhang, and Xiang Bai. Textmonkey: An ocr-free large multimodal model for understanding document. *arXiv preprint arXiv:2403.04473*, 2024d.

Zhuang Liu, Hanzi Mao, Chao-Yuan Wu, Christoph Feichtenhofer, Trevor Darrell, and Saining Xie. A convnet for the 2020s. In *CVPR*, 2022.

Haoyu Lu, Wen Liu, Bo Zhang, Bingxuan Wang, Kai Dong, Bo Liu, Jingxiang Sun, Tongzheng Ren, Zhuoshu Li, Hao Yang, Yaofeng Sun, Chengqi Deng, Hanwei Xu, Zhenda Xie, and Chong Ruan. Deepseek-vl: Towards real-world vision-language understanding, 2024a. URL <https://arxiv.org/abs/2403.05525>.

Pan Lu, Hritik Bansal, Tony Xia, Jiacheng Liu, Chunyuan Li, Hannaneh Hajishirzi, Hao Cheng, Kai-Wei Chang, Michel Galley, and Jianfeng Gao. Mathvista: Evaluating mathematical reasoning of foundation models in visual contexts. In *ICLR*, 2024b.

Gen Luo, Yiyi Zhou, Yuxin Zhang, Xiaowu Zheng, Xiaoshuai Sun, and Rongrong Ji. Feast your eyes: Mixture-of-resolution adaptation for multimodal large language models, 2024. URL <https://arxiv.org/abs/2403.03003>.

Ahmed Masry, Do Xuan Long, Jia Qing Tan, Shafiq Joty, and Enamul Hoque. Chartqa: A benchmark for question answering about charts with visual and logical reasoning, 2022. URL <https://arxiv.org/abs/2203.10244>.

Minesh Mathew, Viraj Bagal, Rubèn Pérez Tito, Dimosthenis Karatzas, Ernest Valveny, and C. V. Jawahar. Infographicvqa, 2021a. URL <https://arxiv.org/abs/2104.12756>.

Minesh Mathew, Dimosthenis Karatzas, and C. V. Jawahar. Docvqa: A dataset for vqa on document images, 2021b. URL <https://arxiv.org/abs/2007.00398>.

Alec Radford, Jong Wook Kim, Chris Hallacy, Aditya Ramesh, Gabriel Goh, Sandhini Agarwal, Girish Sastry, Amanda Askell, Pamela Mishkin, Jack Clark, Gretchen Krueger, and Ilya Sutskever. Learning transferable visual models from natural language supervision, 2021. URL <https://arxiv.org/abs/2103.00020>.

Samyam Rajbhandari, Jeff Rasley, Olatunji Ruwase, and Yuxiong He. Zero: Memory optimizations toward training trillion parameter models, 2020. URL <https://arxiv.org/abs/1910.02054>.

Christoph Schuhmann, Romain Beaumont, Richard Vencu, Cade Gordon, Ross Wightman, Mehdi Cherti, Theo Coombes, Aarush Katta, Clayton Mullis, Mitchell Wortsman, Patrick Schramowski, Srivatsa Kundurthy, Katherine Crowson, Ludwig Schmidt, Robert Kaczmarczyk, and Jenia Jitsev. Laion-5b: An open large-scale dataset for training next generation image-text models, 2022. URL <https://arxiv.org/abs/2210.08402>.

Amanpreet Singh, Vivek Natarajan, Meet Shah, Yu Jiang, Xinlei Chen, Dhruv Batra, Devi Parikh, and Marcus Rohrbach. Towards vqa models that can read, 2019. URL <https://arxiv.org/abs/1904.08920>.

Rubèn Tito, Dimosthenis Karatzas, and Ernest Valveny. Document collection visual question answering. In *ICDAR* 2021, 2021.

Hugo Touvron, Thibaut Lavril, Gautier Izacard, Xavier Martinet, Marie-Anne Lachaux, Timothée Lacroix, Baptiste Rozière, Naman Goyal, Eric Hambro, Faisal Azhar, Aurelien Rodriguez, Armand Joulin, Edouard Grave, and Guillaume Lample. Llama: Open and efficient foundation language models, 2023. URL <https://arxiv.org/abs/2302.13971>.

A Vaswani. Attention is all you need. *Advances in Neural Information Processing Systems*, 2017.

Haoran Wei, Lingyu Kong, Jinyue Chen, Liang Zhao, Zheng Ge, Jinrong Yang, Jianjian Sun, Chunrui Han, and Xiangyu Zhang. Vary: Scaling up the vision vocabulary for large vision-language models, 2023. URL <https://arxiv.org/abs/2312.06109>.

Ruyi Xu, Yuan Yao, Zonghao Guo, Junbo Cui, Zanlin Ni, Chunjiang Ge, Tat-Seng Chua, Zhiyuan Liu, Maosong Sun, and Gao Huang. Llava-uhd: an lmm perceiving any aspect ratio and high-resolution images. *arXiv preprint arXiv:2403.11703*, 2024.

Jiabo Ye, Anwen Hu, Haiyang Xu, Qinghao Ye, Ming Yan, Guohai Xu, Chenliang Li, Junfeng Tian, Qi Qian, Ji Zhang, et al. Ureader: Universal ocr-free visually-situated language understanding with multimodal large language model. *arXiv preprint arXiv:2310.05126*, 2023.

Qinghao Ye, Haiyang Xu, Jiabo Ye, Ming Yan, Anwen Hu, Haowei Liu, Qi Qian, Ji Zhang, and Fei Huang. mplug-owl2: Revolutionizing multi-modal large language model with modality collaboration. In *Proceedings of the IEEE/CVF Conference on Computer Vision and Pattern Recognition*, pp. 13040–13051, 2024.

Xiang Yue, Yuansheng Ni, Kai Zhang, Tianyu Zheng, Ruoqi Liu, Ge Zhang, Samuel Stevens, Dongfu Jiang, Weiming Ren, Yuxuan Sun, Cong Wei, Botaq Yu, Ruibin Yuan, Renliang Sun, Ming Yin, Boyuan Zheng, Zhenzhu Yang, Yibo Liu, Wenhao Huang, Huan Sun, Yu Su, and Wenhui Chen. Mmmu: A massive multi-discipline multimodal understanding and reasoning benchmark for expert agi. In *CVPR*, 2024.

Xiaohua Zhai, Basil Mustafa, Alexander Kolesnikov, and Lucas Beyer. Sigmoid loss for language image pre-training, 2023. URL <https://arxiv.org/abs/2303.15343>.

Susan Zhang, Stephen Roller, Naman Goyal, Mikel Artetxe, Moya Chen, Shuohui Chen, Christopher Dewan, Mona Diab, Xian Li, Xi Victoria Lin, Todor Mihaylov, Myle Ott, Sam Shleifer, Kurt Shuster, Daniel Simig, Punit Singh Koura, Anjali Sridhar, Tianlu Wang, and Luke Zettlemoyer. Opt: Open pre-trained transformer language models, 2022. URL <https://arxiv.org/abs/2205.01068>.

Yanzhe Zhang, Ruiyi Zhang, Jiuxiang Gu, Yufan Zhou, Nedim Lipka, Diyi Yang, and Tong Sun. Llavav: Enhanced visual instruction tuning for text-rich image understanding, 2024. URL <https://arxiv.org/abs/2306.17107>.

Dehua Zheng, Wenhui Dong, Hailin Hu, Xinghao Chen, and Yunhe Wang. Less is more: Focus attention for efficient detr. In *Proceedings of the IEEE/CVF international conference on computer vision*, pp. 6674–6683, 2023.

Chunting Zhou, Pengfei Liu, Puxin Xu, Srinivas Iyer, Jiao Sun, Yuning Mao, Xuezhe Ma, Avia Efrat, Ping Yu, Lili Yu, Susan Zhang, Gargi Ghosh, Mike Lewis, Luke Zettlemoyer, and Omer Levy. Lima: Less is more for alignment, 2023. URL <https://arxiv.org/abs/2305.11206>.

Deyao Zhu, Jun Chen, Xiaoqian Shen, Xiang Li, and Mohamed Elhoseiny. Minigpt-4: Enhancing vision-language understanding with advanced large language models. *arXiv preprint arXiv:2304.10592*, 2023.

A MORE VISUALIZATION

We selected images from DocVQA, WikiTableQuestions, and TextVQA, designed questions, and shifted the images so that the answers are at the edge of the cropped boundary. We compared our model with Minigemini-HD and LLaVA-NeXT. As shown in Figure 5, our model’s performance in answering at the cropped boundary is mostly correct, while both Minigemini-HD and LLaVA-NeXT provided incorrect answers.

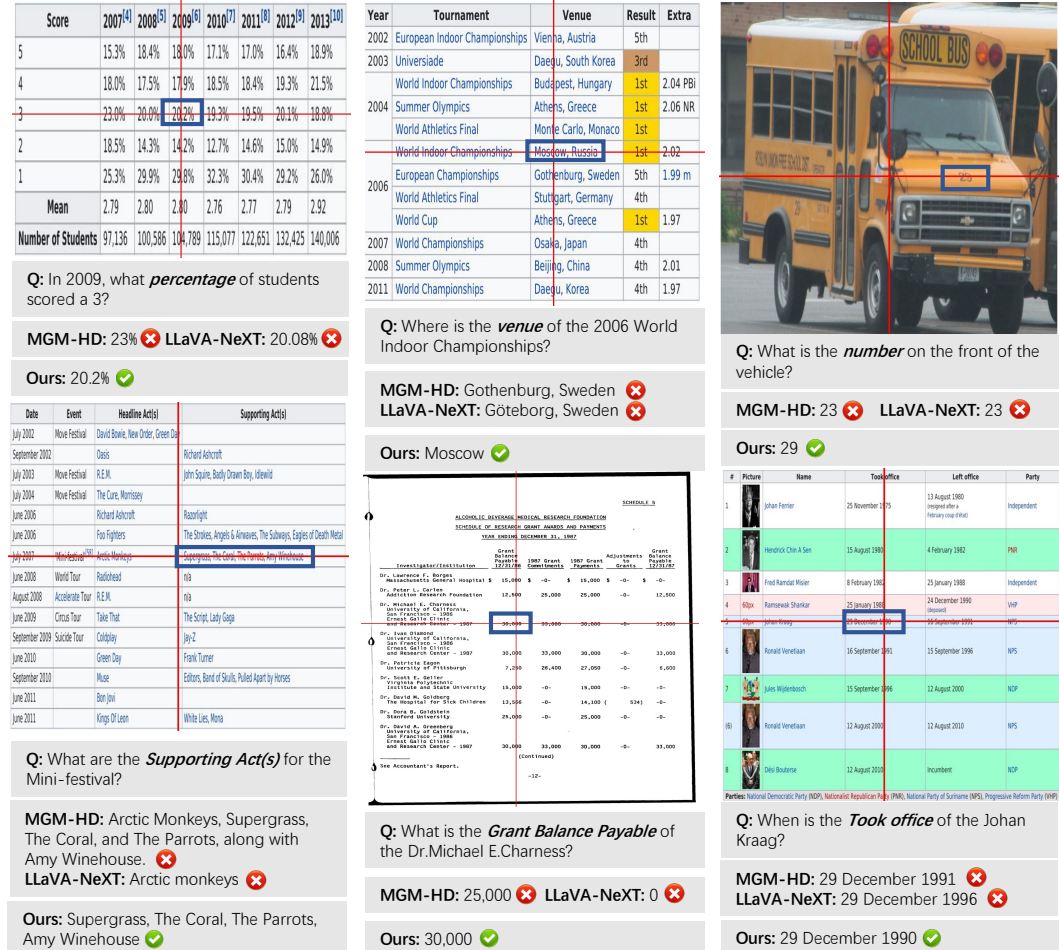


Figure 5: Qualitative results. The red solid line in the image represents the cropping boundary, and the blue box indicates the location of the answer. All images are sized at 672 × 672. Neither the red solid line nor the blue box will be input into the model.

B TRAINING SETTINGS

In this study, we use the ViT-L pretrained by CLIP (Radford et al., 2021) and ConvNeXt-L pretrained by LAION (Schuhmann et al., 2022) as the high-resolution visual encoder and the main architecture of Hybrid Encoder, respectively. For the language model, we utilize LLaMA3-8B-Instruct (Touvron et al., 2023). We optimize the model for 1 epoch using the AdamW optimizer with a cosine learning rate schedule and a warmup ratio of 0.03. During the pretraining stage, we use a peak learning rate of 1e-3 and a batch size of 256, training the projection and interaction layers. In the instruction fine-tuning phase, our main peak learning rate is 1e-5 with a batch size of 64. The learning rate for the visual encoder is reduced to 2e-6 to ensure stability, while the interaction layer remains at 1e-5. We employ the DeepSpeed Zero (Rajibhandari et al., 2020) 2 strategy, completing the optimization in a total of 32 hours on 32 × A800 GPUs.

C ALIGNMENT STRATEGY

Conv Stage	Input Dimensions (D, H, W)	Output Dimensions (D, H, W)	ViT Layer	ViT Dimensions (D, H, W)
1	(192, 192, 192)	(3072, 24, 24)	2	(1024, 24, 24)
2	(384, 96, 96)	(1536, 24, 24)	6	(1024, 24, 24)
3	(768, 48, 48)	(3072, 24, 24)	12	(1024, 24, 24)
4	(1536, 24, 24)	(1536, 24, 24)	20	(1024, 24, 24)

Table 5: Alignment Strategy. The alignment strategy ultimately aims to ensure that ConvNeXT aligns with the hidden states of CLIP-ViT along the H and W dimensions, allowing concatenation along the channel dimension.

In the ConvNeXT-ViT Deep Fusion Module, we opted for channel concatenation. Table 5 provides a detailed illustration of the dimensional changes in the features at different stages of ConvNeXT and the corresponding interaction layers with CLIP-ViT. Here, we use an image with a resolution of 372×372 as an example. According to the cropping strategy, the resolution of the images input into ConvNeXT will be 768×768 .